PET/MRI in Cervical Cancer

Subjects: Oncology
Contributor: Mayur Virarkar , Sai Swarupa Vulasala , Luis Calimano-Ramirez , Anmol Singh , Chandana Lall , Priya Bhosale

Early detection of gynecological malignancies is vital for patient management and prolonging the patient's survival. Molecular imaging, such as positron emission tomography (PET)/computed tomography, has been increasingly utilized in gynecological malignancies. PET/magnetic resonance imaging (MRI) enables the assessment of gynecological malignancies by combining the metabolic information of PET with the anatomical and functional information from MRI. Cervical cancer is one of the tumors that demonstrate heterogeneity to hypoxia. PET/MRI has been established to assess the tumor response in cervical cancer, and its capability is questionable in the case of ovarian tumors.

PET/MRI gynecological malignancy PET/CT

1. Epidemiology

Uterine cervical cancer is the fourth most common cancer worldwide, with roughly 604,127 cases diagnosed and an annual mortality of 341,831 [1][2]. About 80–90% of the cases described are encountered in developing countries due to the lack of proper screening practices [3]. On the other hand, the incidence has drastically reduced in the United States due to robust screening with pap smear exams and Human Papilloma Virus (HPV) DNA testing and cases hae remained stable during the recent decade (2009–2018). It is estimated that 14,100 new cases and 4280 deaths of invasive cervical cancer will be observed in the United States in 2022 [4]. The survival rate, in general, has been reported as 66%. However, it is lower (39%) in African American women of age ≥65 years [4].

2. Classification

Most cervical cancers arise from the junctional zone between the cervix's outer squamous and inner columnar epithelial lining. According to World Health Organization (WHO) classification, cervical cancer can be of various histologic subtypes: (i) squamous cell carcinoma (SCC), (ii) adenocarcinoma, (iii) clear cell adenocarcinoma, (iv) adenosquamous carcinoma, (v) serous carcinoma, (vi) glassy cell carcinoma, (vii) adenoid basal carcinoma, (viii) adenoid cystic carcinoma, (ix) undifferentiated carcinoma, and (x) adenocarcinoma [5]. The SCC constitutes 75% of cervical cancer encounters, while the adenocarcinoma comprises 10–25%, adenosquamous 20%, and the rest of the histologies <5% of cases [3][5]. The dysplastic lesions of SCC can be divided into high-grade squamous intraepithelial lesions (HGSIL) and low-grade squamous intraepithelial lesions (LGSIL).

3. Imaging

Although the previous FIGO classifications did not include the imaging criteria for tumor staging, the 2018 classification has permitted the utility of imaging, which enabled better tumor assessment and staging [2][6][7]. The FIGO staging was based on clinical evaluation due to a limited access to imaging in low-income countries with high cervical cancer prevalence [8]. However, clinical staging is suboptimal for certain tumor characteristics such as size, parametrial invasion, and lymph node involvement. In patients with early-stage cervical cancer (IA and part of IB1), the microinvasion is only detectable using tissue evaluation [9]. The rest of the tumor stages, including local extension, can be assessed using reliable imaging modalities such as CT, MRI, and PET/CT, which have higher sensitivity and comparable specificity to the clinical evaluation [10][11]. The National Comprehensive Cancer Network 2022 Practice Guidelines in Oncology recommended CT or PET/CT for tumor surveillance and follow-up, and MRI for the local assessment of the stage ≥ IB1 [8][12]. Staging is essential to predict survival, and surgical planning is considered standard management for early-stage (≤IIA) cervical cancers [13]. Nguyen et al. compared PET/CT and PET/MRI and found that both modalities could identify all the primary and metastatic lesions and could strongly correlate standardized uptake value (SUV) (p = 0.03) [12] (**Figure 1**).

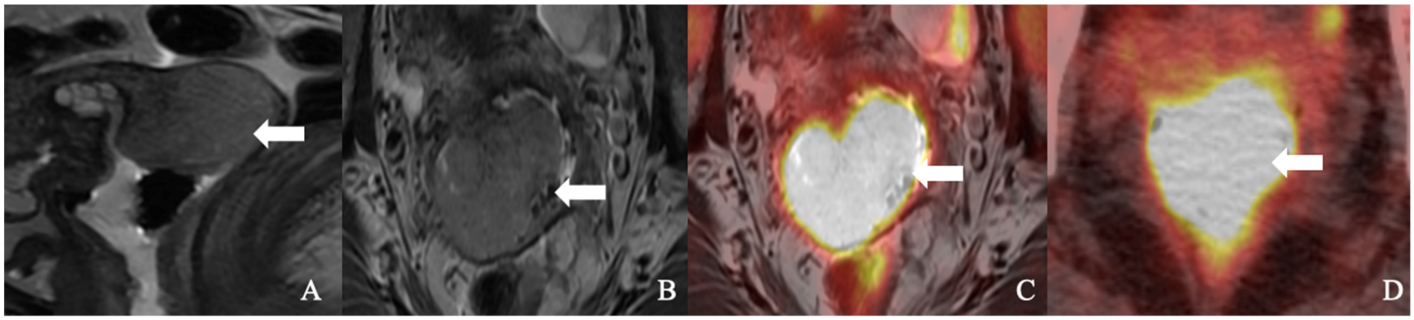

Figure 1. A 51-year-old woman with squamous cell carcinoma of the cervix. (**A**). Sagittal T2-weighted imaging (T2WI), (**B**). axial T2WI, and (**C**). axial fused T2WI positron emission tomography/MRI showing a large (18)F-fluorodeoxyglucose (FDG) avid cervical mass (arrow). (**D**). An axial positron emission tomography/computed tomography image showed FDG avidity cervical tumor (arrow).

In general, diffusion weighted imaging (DWI) is considered sensitive to assessing parametrial involvement. It has high false-positive rates if the patients have large tumor sizes or a superimposed infections. Imaging must be highly specific to demonstrate the local tumor invasion since the curative surgery can be performed based on the parametrial invasion [13]. Moreover, identifying stromal, ovarian, or corpus invasion is crucial as they are risk factors for lymphovascular space invasion (LVSI) and para-aortic lymph nodal metastases [14][15].

The successful integration of PET and MRI enabled tumor evaluation and staging in a “one-stop” approach. In a study by Steiner et al., PET/MRI has proven to have a benefit over MRI with an Area Under Curve (AUC) of 0.85 vs. 0.74 for vaginal invasion and 0.89 vs. 0.73 for parametrial invasion [13]. Similar findings were observed in the study by Sarabhai et al., who reported that PET/MRI and MRI are similar in characterizing the T-stage of the tumor (85% vs. 87%) [16]. Wang et al. reported that PET/MRI has a sensitivity, specificity, and negative predictive value

(NPV) of 78.5%, 64.9%, and 74.5%, respectively, compared to MRI [17]. PET/MRI characterizes the parametrial invasion with a sensitivity and specificity of 90% and 94% [17]. Kitajima et al. reported a diagnostic accuracy of 83% compared to MRI alone in a study comprising 30 patients [18].

All the studies above were based on morphological observations on PET/MRI. Instead, Wang et al. quantified the gray level values to evaluate the parametrial invasion. They reported that high gray values corresponded to the higher FIGO stages ($p < 0.05$); hence, this quantification technique is practical to implement in clinical practice [17]. Wang et al. described the sensitivity, specificity, and NPV of combined PET/MRI+ gray values as 87%, 84%, and 86%, respectively, compared to MRI or PET/MRI alone, in assessing parametrial invasion ($p < 0.05$) [17].

The tumor cells drain from the cervix, through the lymphatic vessels, into parametrial lymph nodes, pelvic sidewall nodes, external and internal iliac nodes, and para-aortic nodes [19]. Around 10–30% of patients with cervical cancer demonstrate pelvic lymph node metastases (LNM) during an early stage. This reduces the 5-year survival rate from 94.1% (negative LNM) to 64.1% (positive LNM) [20]. Accurate lymph nodal assessment is essential for developing the individualized treatment algorithm, enhancing the prognosis, and reducing mortality. According to FIGO 2018 classification, micro- or macro-metastases to the lymph nodes are staged as IIIC regardless of tumor size or extent [21]. CT and MRI are less sensitive and specific in detecting metastatic lymph nodes, as they cannot differentiate metastatic from non-metastatic lymph nodes [22][23]. The combined PET/CT was studied, which showed high sensitivity (91% vs. 37.3%) and diagnostic accuracy (98% vs. 95%) compared to MRI ($p < 0.034$), and hence is recommended by the National Comprehensive Cancer Network clinical guidelines [23][24]. However, the PET is limited by identifying small lymph nodal metastases of size < 5 mm [25]. Later, PET/MRI was found to have improved diagnostic confidence over PET/CT with the advantage of a reduced radiation dose [26] (**Figure 2**). PET/MRI has a sensitivity, specificity, and diagnostic accuracy of 91%, 94%, and 93% in detecting nodal metastases [12]. Compared to PET/CT, PET/MRI identifies nodal metastases with a sensitivity, specificity, and accuracy of 92.3%, 88.2%, and 90%, respectively [18].

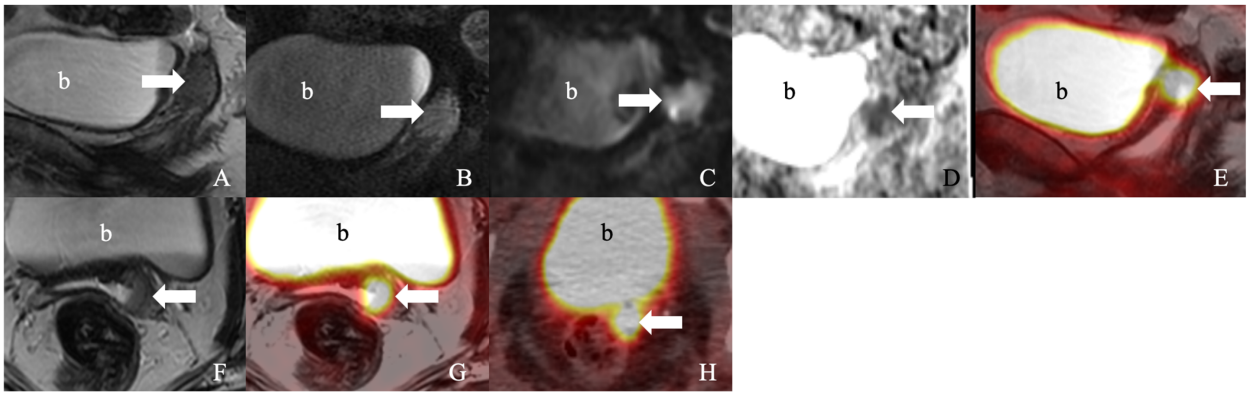

Figure 2. A 55-year-old woman with squamous cell carcinoma of the cervix, status post hysterectomy. (**A**). Sagittal T2-weighted imaging (T2WI), (**B**). post-contrast sagittal T1-weighted imaging (T1WI), (**C**). coronal diffusion-weighted image (DWI), (**D**). coronal apparent diffusion coefficient (ADC), (**E**). coronal fused T2WI, and (**F**). axial T2WI. (**G**). Axial fused T2WI positron emission tomography/MRI showed an enhancing (18)F-fluorodeoxyglucose

(FDG) avid plaque-like thickening at the left cervix (arrow) with restricted diffusion. (**H**). An axial positron emission tomography/computed tomography image showed ill-defined FDG avidity (arrow). b: urinary bladder.

Cervical cancer is one of the tumors that demonstrate heterogeneity to hypoxia. Narva et al. studied the association between hypoxia and increased resistance to chemotherapy and radiotherapy in patients with SCC of the cervix [27][28]. In addition, the cancerous cells adapt to the hypoxic microenvironment, leading to genetic instability, DNA damage, and mutagenesis. This results in a rapid tumor invasion to the adjacent and distant organs. ^{18}Fluorine-labeled 2-(2-nitro-1-*H*-imidazol-1-y)-*N*-(2,2,3,3,3-pentafluoropropyl)-acetamide (^{18}F-EF5) is a hypoxia radiotracer that can be used in PET imaging. Increased uptake of ^{18}F-EF5 is strongly associated with poor prognosis compared to (18)F-fluorodeoxyglucose (^{18}F-FDG) uptake. Narva et al. reported that an increased ^{18}F-EF5 uptake on ^{18}F-EF5-PET/MRI correlates with hypoxia intensity, which is proportional to the tumor stage [27].

Radiotherapy is the cornerstone in the management of patients with cervical cancer. Around 25% of cervical cancer cases recur, and 24% among those are observed in already-treated patients, which points to the importance of identifying the radio-resistant tumor areas that may be managed with radiation dose escalation. A new PET tracer ^{68}Ga-NODAGA-E[c(RGDyK)]2 ([^{68}Ga] (Ga-RGD)) identifies the $\alpha_v\beta_3$, an integrin that is found on the newly formed vasculature. Pelvic insufficiency fractures (PIF) are a late complication of radiotherapy, and Sapienza et al. studied the incidence of PIF in patients who underwent radiotherapy for various gynecologic cancers [29]. They found that 10–18% of patients are affected by PIF, with the sacrum as the most common fracture site [29]. Azumi et al. noticed PIF in 20% of patients with cervical cancer treated with radiotherapy [30]. They also demonstrated that PET/MRI discovers PIF earlier than PET/CT (p <0.05), with the added advantage of reduced radiation exposure [30]. The earliest sign of PIF is medullary edema, which can be observed as T1 hypointense and T2 hyperintense on MRI as early as 18 days after the symptom onset [30].

The maximum standardized uptake value (SUV_{max}) derived from [^{18}F] FDG-PET and diffusion metrics such as the apparent diffusion coefficient (ADC) from the MRI are studied as the prognostic indicators in patients with cervical cancer [28][31][32][33][34][35][36][37]. Many studies reported that SUVmax and ADC minimum (ADC_{min}) values of cervical cancer are inversely related. Olsen et al. also described reduced ADC value in intense SUV_{max} [38]. In addition, the SUVmax was seen to vary based on the histology and degree of differentiation of cervical cancer, and this feature aided in the prognostication [39]. SCC of the cervix is found to have higher SUV_{max} values than the non-squamous tumors (p = 0.153), and poorly differentiated ones have higher SUVmax than do the well-differentiated tumors (p = 0.0474) [39]. The underlying reason for the difference in SUVmax is secondary to the degree of Glucose Transporter (Glut) expression that aids in FDG uptake; however, it still needs to be validated through further studies [40][41].

The simultaneous acquisition of PET/MRI provides precise spatial correlation and a more appropriate insight into the imaging biomarkers on the voxel level. The inverse correlation between SUV_{mean}, SUV_{max}, and ADC_{min} was also supported by Brandmaier et al. on hybrid PET/MRI. The correlations between SUV_{mean} and ADC_{min} (r = −0.403) and SUV_{max} and ADC_{min} (r = −0.532) were significant in primary cervical tumors [42]. The authors demonstrated a stronger correlation between SUV_{mean} and ADC_{min} (r = 0.773) and SUV_{max} and ADC_{min} (r =

−0.747) in the case of recurrent cervical tumors [42]. Grueneisen et al. reported significant SUVmax and ADC_{min} in primary tumors but not the recurrent cervical tumors [43]. Later, Ho et al. described no correlation among SUV_{max}, SUV_{mean}, ADC_{min}, or ADC_{mean}. However, they found that the ratio of ADC_{min}/ADC_{mean} (relative admin) and the ratio of SUV_{max} and SUV_{mean} (relative SUV_{max}) correlated well with the adeno- and adenosquamous carcinoma of the cervix (r = −0.685) and with the well- to moderately differentiated tumors (r = −0.631) [44]. No significant correlation between relative SUVmax and relative ADC_{min} was found in squamous cell carcinoma and poorly differentiated tumors [44]. Surov et al. studied the SUV and ADC parameters and their relation with the KI 67 proliferation index [45]. They found that SUVmax (r = 0.59), SUV_{mean} (r = 0.45), SUV_{max}/ADC_{min} (r = 0.71), SUV_{max}/ADC_{mean} (r = 0.75), and ADC_{min} (r = −0.48) correlated significantly with the KI 67 proliferative index, thereby reflecting the tumor proliferation rate [45]. Additionally, SUV_{mean} (r = 0.71) and SUV_{max} (r = −0.71) strongly correlate with epithelial and stromal areas and locate the metabolically active areas [45]. In addition to SUV and ADC, the other parameters include metabolic tumor volume (MTV) and total lesion glycolysis (TLG). It has been studied that these parameters conventionally correlate with the SCC antigen levels, FIGO staging, tumor size, and depth of stromal invasion [46] [47]. **Table 1** and **Table 2** summarize the essential characteristics of PET/MRI studies in cervical and pelvic malignancies.

Table 1. Characteristics of PET/MRI studies in cervical cancer.

Serial Number	Study	Year of Publication	Type of Study	Total Patient Number	Objective of Study	PET MRI Machine Details	Result	Limitations
1	Floberg et al. [48]	2018	Retrospective	17	To describe the relation between ADC and SUV values on MRI and PET imaging, respectively.	nMR-integrated PET/MRI	SUV_{mean} and ADC_{mean} (p = 0.007) and SUV_{mean} and $ADC_{T/M}$ (p = 0.008) are inversely correlated. Such inverse correlation was not statistically significant when the tumors were divided into Adenocarcinomas and SCC.	Retrospective study with small sample size; Heterogeneous patient cohort including patients treated with surgery or chemoradiation and cancers of varied sizes, grades, histology, and stages.
2	Nguyen et al. [12]	2020	Prospective	6	To compare the diagnostic performance of FDG PET/MRI vs. PET/CT.	Discovery 710 PET/CT and Biograph mMR 3T scanner	There is a strong correlation between the tumor SUVs on PET/CT and PET/MRI (p < 0.001). PET/MRI has superior	Small sample size; Lack of histological confirmation and correlation; Confounding bias as a result of the time gap

Serial Number	Study	Year of Publication	Type of Study	Total Patient Number	Objective of Study	PET MRI Machine Details	Result	Limitations
							diagnostic interpretation and identified 4 of the 6 tumors not identified on PET/CT.	between the two imaging methods
3	Surov et al. [45]	2017	Prospective	21	To study the relation between ADC and SUV values, and their importance in estimating tumor proliferation (KI 67).	Biograph mMR PET/MRI	SUV_{max} (p = 0.005), SUV_{mean} (p = 0.04), ADC_{min} (p = 0.03), SUV_{max}/ADC_{min} (p = 0.001), and $SUVmax/ADC_{mean}$ (p = 0.001) are significantly correlated with KI-67	Small sample size
4	Anner et al. [23]	2016	Retrospective	27	To study the quality of MRI, PET/CT, and PET/MRI in the lymph nodal staging of cervical carcinoma. Authors compared the diagnostic efficacy of imaging compared to histological analyses.	64-row multidetector PET/CT, Magnetom trio 3-T MRI; PET/MRI images were reconstructed virtually from individual MRI and PET/CT images	PET/MRI has similar sensitivity (64%) and moderate specificity (77% vs. 69%), PPV (75% vs. 69%), and NPV (67% vs. 64%) compared to PET/CT images. Hence, the study concluded that PET/MRI is not superior to PET/CT in the lymph nodal staging of cervical cancer patients.	Small population; Retrospective study design; Discrepancy between the imaging and histological analyses; Virtually reconstructed PET/MRI images rather than originally obtained scanner images.
5	Wang et al. [17]	2019	Retrospective	79	To study the diagnostic efficacy of integrated PET/MRI in identifying the parametrial involvement and the importance of gray value while interpreting PET/MRI.	Signa PET/MRI (Integrated scanner)	The accuracy, sensitivity, and NPV of PET/MRI are higher than conventional MRI; however, it was not significant (p = 1.0). The accuracy, sensitivity, and NPV of combined	Retrospective analysis resulting in selection bias; Small sample size; No evaluation between multiple observers.

Serial Number	Study	Year of Publication	Type of Study	Total Patient Number	Objective of Study	PET MRI Machine Details	Result	Limitations
							PET/MRI+ gray values are significantly superior to conventional MRI ($p < 0.05$).	
6	Narva et al. [27]	2021	Prospective	9	To evaluate the correlation between PET/MRI imaging (^{18}F-EF5) and endogenous hypoxia (such as HIF1, CAIX, and GLUT1) tracers.	Ingenuity TF PET/MRI	18F-EF5 max T/M ratio ($p = 0.036$) and HSV ($p = 0.040$) correlated with advanced-stage tumors and HSV correlated with tumor size ($p = 0.02$).	Small sample size; the chemistry of EF5 is complex, which may limit its broad application.
7	Brandmaier et al. [42]	2015	Prospective	31	To study the correlation between ADC and SUV values on simultaneous PET/MRI and their importance in primary and recurrent cervical cancer.	Magnetom Biograph mMR PET/MRI scanner	There was a significant inverse correlation between ADCmin and SUVmax ($p = 0.05$) and SUVmean and ADCmin ($p = 0.03$) in patients with primary tumors, primary metastases, and recurrent tumors ($p = 0.002$); No significant correlation among patients with recurrent metastases ($p > 0.05$).	Histopathological correlation was not performed; Included are the visible lesions on both imaging modalities; Average uptake time for FDG on PET/MRI is approximately 30 min, which could affect the SUV measurements.
8	Umutlu et al. [49]	2020	Prospective	30	To evaluate if PET/MRI can identify N- and M-staging of primary cervical cancers and, based on the results, if it can be a platform for radiomics analysis and artificial	Biograph mMR PET/MRI scanner	PET/MRI is superior in determining the M-stage than the N-stage, with a sensitivity and specificity of 91% and 92%, respectively. AUC was 0.97 for the M-staging and	Small patient cohort; Heterogeneous histopathology and tumor sizes.

Serial Number	Study	Year of Publication	Type of Study	Total Patient Number	Objective of Study	PET MRI Machine Details	Result	Limitations
					intelligence algorithms.		0.82 for the N-staging.	
9	Meyer et al. [50]	2018	Prospective	18	To study the correlation between the parameters of cervical cancer's histopathology and PET/MRI imaging.	Biograph mMR PET/MRI scanner	Authors identified no significant correlation between SUVmax, SUVmean, and ADC histogram parameters; Total lesion glycolysis was correlated inversely with p25, p75, p90, ADCmedian, and ADCmode. MTV also significantly corelated with ADCmean, p10, p25, p75, p90, ADCmedian, and ADCmode.	Retrospective study; Small sample size; Only squamous cell carcinomas were evaluated.
10	Sarabhai et al. [16]	2017	Prospective	53	To compare the efficacy of PET/MRI and MRI alone for evaluating primary and metastatic cervical tumors.	Biograph mMR whole-body PET/MRI scanner	T-staging: PET/MRI vs. MRI alone classified 85% vs. 87% of tumors ($p > 0.1$); N-staging: Sensitivity, specificity, and accuracy of PET/MRI were 83%, 90%, and 87%, respectively, and that of MRI alone were 71%, 83%, and 77%, respectively ($p > 0.05$); M-staging: Sensitivity, specificity, and accuracy of PET/MRI were 87%, 92%, and 91%, respectively, while that of MRI alone were 67%,	Small patient cohort and statistical power; Authors used restricted reference standards for all suspicious lesions.

Serial Number	Study	Year of Publication	Type of Study	Total Patient Number	Objective of Study	PET MRI Machine Details	Result	Limitations
							90%, and 83%, respectively (p > 0.05).	
11	Steiner et al. [13]	2021	Retrospective	33	To compare the efficiency of PET/MRI and MRI alone; Role of ADC and SUV values in primary cervical cancer.	Hybrid 3T Ingenuity TF PET/MRI scanner on a phased-array SENSE XL	PET/MRI has higher AUC compared to MRI alone in detecting deep stromal invasion (0.96 vs. 0.74), parametrial invasion (0.89 vs. 0.73), and vaginal invasion (0.85 vs. 0.74); PET/MRI is more sensitive than MRI alone in ruling out residual tumors after radical cone biopsy or hysterectomy (89% vs. 44%); PET/MRI has equal AUC to MRI alone in pelvic nodal staging (0.73 vs. 0.73) but not distant metastases (0.80 vs. 0.67).	Retrospective study; Small cohort; ADC values were obtained from ROI-based mean, rather than whole tumor volume.
12	Vojtisek et al. [51]	2021	Retrospective	66	To identify the role of PET/MRI in predicting tumor treatment response to chemoradiotherapy.	Biograph mMR PET/MRI scanner	The PET/MRI parameters, including mid-MTV, mid-TLG, mid-TLG-S, mid-MTV-s, mid-tumor size, and change in % SUVmax, were significantly different between the responders and non-responders. Of all the parameters, mid-MTV-s showed moderate discrimination	Small cohort; Shorter follow-up interval.

Serial Number	Study	Year of Publication	Type of Study	Total Patients in Study	Objective	PET MR Machine Details	Result	Limitations
1	Xin et al. [56]	2016	Prospective	45	To evaluate the diagnostic performance of PET/MRI in abdominal and pelvic tumors	Discovery 690 PET/CT; Ingenuity TF PET/MRI scanner	There was no significant difference in tumor identification on PET/CT and PET/MRI (p = 0.18); However,	PET/MRI was obtained 105 min after PET/CT, which might have led to physical decay and tracer biokinetics; The position of arms

Serial Number	Study	Year of Publication	Type of Study	Total Patients in Study	Objective	PET MR Machine Details	Result	Limitations
					compared to PET/CT.		PET/MRI images had better quality than PET/CT; There was an excellent correlation of SUV value to the focal lesions (R = 0.948).	varied between the PET/CT and PET/MRI, which could be the reason for the difference in image quality.
2	Queiroz et al. [57]	2015	Prospective	26	To study the role of PET/CT and PET/MRI in staging and re-staging of advanced gynecological cancers.	Discovery PET/CT 690; the fusion was performed on the Advantage workstation	PET/MRI is superior to PET/CT for primary tumor identification ($p < 0.001$). No difference was found in the evaluation of lymph nodes and abdominal metastases.	Small patient population; PET/MRI was not obtained from whole-body imaging.
3	Spick et al. [58]	2016	Retrospective	69	To study whether PET/MRI has improved diagnostic performance in cancer assessment.		PET/MRI has similar diagnostic accuracy as PET/CT in the detection of primary and recurrent pelvic cancers; However, the diagnostic confidence of PET/MRI is higher than PET/CT in benign ($p < 0.05$) and malignant ($p < 0.01$) lesions. In addition,	

Serial Number	Study	Year of Publication	Type of Study	Total Patients in Study	Objective	PET MR Machine Details	Result	Limitations
							lesion conspicuity was better on PET/MRI compared to PET/CT.	
4	Grueneisen et al. [59]	2014	Prospective	48	To study the role of DWI in PET/MRI imaging for primary and recurrent tumor evaluation.	Biograph mMR 3-T PET/MRI scanner	There was no significant effect of DWI on the diagnostic performance of PET/MRI ($p > 0.05$); In fact, higher diagnostic confidence was noted with PET than with the DWI ($p < 0.05$).	Included 48 patients; however, further studies are required to validate the results. Image and histopathological correlation were performed using restricted reference standards.
5	Schwartz et al. [60]	2018	Prospective	18	To compare the diagnostic ability of PET/MRI to PET/CT for patients with gynecologic malignancy.	Biograph mCT PET/CT scanner; Biograph mMR 3-T PET/MRI scanner	PET/CT and PET/MRI have similar diagnostic potential in visualizing the regional lymph nodes and abdominal metastases, whereas PET/MRI is more sensitive than PET/CT in demonstrating the soft-tissue involvement.	Small cohort; Heterogeneous sample; PET/MRI was limited to only abdominopelvic cavity.
6	Nakajo et al. [61]	2010	Retrospective	31	To compare the diagnostic accuracy of FDG PET/CT	Fusion of PET/CT and MRI images was	PET/T2W MRI images localized the lesion better than the	Misregistration secondary to motion artifact between PET and MRI; Pelvis

obal
6

efficient;
ess; CT:

Co[illegible] 2019, 44, 2557–2571. Positive Predictive Value; NPV: Negative Predictive Value; 18F-EF5: ^{18}Fluorine-labeled 2-(2-nitro-1-*H*-imidazol-1-y)-*N*-(2,2,3,3,3-pentafluoropropyl)-acetamide; HIF1: Hypoxia-Inducible Factor 1; CAIX: Carbonic Anhydrase; GLUT1: Glucose Transporter; 18F-EF5 T/M ratio: 18F-EF5 Tumor to Muscle uptake ratio; HSV: Hypoxic subvolume; MTV: Metabolic Tumor Volume; AUC: Area Under the Curve; TLG: Total Lesion Glycolysis; mid-TLG-5 and mid-MTV-5: Midtreatment parameters at week 5 of chemoradiotherapy; sCT: MRI-derived Synthetic CT; PIF: Pelvic Insufficiency Fracture.

3. Balcacer, P.; Shergill, A.; Litkouhi, B. MRI of cervical cancer with a surgical perspective: Staging, prognostic implications and pitfalls. Abdom. Radiol. 2019, 44, 2557–2571.
4. American Cancer Society. Cancer Facts & Figures 2022. Available online: https://www.cancer.org/research/cancer-facts-statistics/all-cancer-facts-figures/cancer-facts-figures-2022.html# (accessed on 1 October 2022).

Serial Number	Study	Year of Publication	Type of Study	Total Patients in Study	Objective	PET MR Machine Details	Result	Limitations
					vs. PET/MRI in gynecological malignancies.	conducted using Osirix imaging software	PET/T1W or PET/CT images during the first ($p < 0.01$), second ($p < 0.01$), and third ($p < 0.01$) evaluation.	MR images, instead of whole-body MR images, were used for fusion images; Only two readers scored the images.

8. Ghani, M.A.; Liau, J.; Eskander, R.; Mell, L.; Yusufaly, T.; Obrzut, S. Imaging Biomarkers and Liquid Biopsy in Assessment of Cervical Cancer. J. Comput. Assist. Tomogr. 2022, 46, 707–715.
9. Tsuyoshi, H.; Tsujikawa, T.; Yamada, S.; Okazawa, H.; Yoshida, Y. Diagnostic Value of 18F-FDG PET/MRI for Revised 2018 FIGO Staging in Patients with Cervical Cancer. Diagnostics 2021, 11, 202.
10. Xiao, M.; Yan, B.; Li, Y.; Lu, J.; Qiang, J. Diagnostic performance of MR imaging in evaluating prognostic factors in patients with cervical cancer: A meta-analysis. Eur. Radiol. 2020, 30, 1405–1418.
11. Thomeer, M.G.; Gerestein, C.; Spronk, S.; van Doorn, H.C.; van der Ham, E.; Hunink, M.G. Clinical examination versus magnetic resonance imaging in the pretreatment staging of cervical carcinoma: Systematic review and meta-analysis. Eur. Radiol. 2013, 23, 2005–2018.
12. Nguyen, N.C.; Beriwal, S.; Moon, C.H.; Furlan, A.; Mountz, J.M.; Rangaswamy, B. F-FDG PET/MRI Primary Staging of Cervical Cancer: A Pilot Study with PET/CT Comparison. J. Nucl. Med. Technol. 2020, 48, 331–335.
13. Steiner, A.; Narva, S.; Rinta-Kiikka, I.; Hietanen, S.; Hynninen, J.; Virtanen, J. Diagnostic efficiency of whole-body 18F-FDG PET/MRI, MRI alone, and SUV and ADC values in staging of primary uterine cervical cancer. Cancer Imaging 2021, 21, 16.
14. Chen, X.L.; Chen, G.W.; Xu, G.H.; Ren, J.; Li, Z.L.; Pu, H.; Li, H. Tumor Size at Magnetic Resonance Imaging Association With Lymph Node Metastasis and Lymphovascular Space Invasion in Resectable Cervical Cancer: A Multicenter Evaluation of Surgical Specimens. Int. J. Gynecol. Cancer 2018, 28, 1545–1552.
15. Ayhan, A.; Aslan, K.; Öz, M.; Tohma, Y.A.; Kuşçu, E.; Meydanli, M.M. Para-aortic lymph node involvement revisited in the light of the revised 2018 FIGO staging system for cervical cancer. Arch. Gynecol. Obstet. 2019, 300, 675–682.
16. Sarabhai, T.; Schaarschmidt, B.M.; Wetter, A.; Kirchner, J.; Aktas, B.; Forsting, M.; Ruhlmann, V.; Herrmann, K.; Umutlu, L.; Grueneisen, J. Comparison of 18F-FDG PET/MRI and MRI for pre-therapeutic tumor staging of patients with primary cancer of the uterine cervix. Eur. J. Nucl. Med. Mol. Imaging 2018, 45, 67–76.

PET—Positron Emission Tomography; MRI, Magnetic Resonance Imaging; ADC, Apparent Diffusion Coefficient; SUV, Standardized Uptake Volume; CT, Computed tomography; FDG, (18)F-fluorodeoxyglucose; DWI, Diffusion Weighted Imaging.

17. Wang, T.; Sun, H.; Han, F.; Sun, W.; Chen, Z. Evaluation of parametrial infiltration in cervical cancer with voxel-based segmentation of integrated 18F-FDG PET/MRI images: A preliminary study. Eur. J. Radiol. 2019, 118, 147–152.
18. Kitajima, K.; Suenaga, Y.; Ueno, Y.; Kanda, T.; Maeda, T.; Deguchi, M.; Ebina, Y.; Yamada, H.; Takahashi, S.; Sugimura, K. Fusion of PET and MRI for staging of uterine cervical cancer: Comparison with contrast-enhanced (18)F-FDG PET/CT and pelvic MRI. Clin. Imaging 2014, 38, 464–469.
19. Wiebe, E.; Denny, L.; Thomas, G. Cancer of the cervix uteri. Int. J. Gynaecol. Obstet. 2012, 119 (Suppl. 2), S100–S109.
20. Wang, M.; Ma, M.; Yang, L.; Liang, C. Development and validation of a nomogram for predicting pelvic lymph node metastasis and prognosis in patients with cervical cancer. Front. Oncol. 2022, 12, 952347.
21. Bhatla, N.; Aoki, D.; Sharma, D.N.; Sankaranarayanan, R. Cancer of the cervix uteri. Int. J. Gynaecol. Obstet. 2018, 143 (Suppl. 2), 22–36.
22. Zigras, T.; Lennox, G.; Willows, K.; Covens, A. Early Cervical Cancer: Current Dilemmas of Staging and Surgery. Curr. Oncol. Rep. 2017, 19, 51.
23. Anner, P.; Mayerhöfer, M.; Wadsak, W.; Geleff, S.; Dudczak, R.; Haug, A.; Hacker, M.; Karanikas, G. FDG-PET/CT and MRI for initial pelvic lymph node staging in patients with cervical carcinoma: The potential usefulness of FDG-PET/MRI. Oncol. Lett. 2018, 15, 3951–3956.
24. Lv, K.; Guo, H.M.; Lu, Y.J.; Wu, Z.X.; Zhang, K.; Han, J.K. Role of 18F-FDG PET/CT in detecting pelvic lymph-node metastases in patients with early-stage uterine cervical cancer: Comparison with MRI findings. Nucl. Med. Commun. 2014, 35, 1204–1211.
25. Sironi, S.; Buda, A.; Picchio, M.; Perego, P.; Moreni, R.; Pellegrino, A.; Colombo, M.; Mangioni, C.; Messa, C.; Fazio, F. Lymph node metastasis in patients with clinical early-stage cervical cancer: Detection with integrated FDG PET/CT. Radiology 2006, 238, 272–279.
26. Beiderwellen, K.; Grueneisen, J.; Ruhlmann, V.; Buderath, P.; Aktas, B.; Heusch, P.; Kraff, O.; Forsting, M.; Lauenstein, T.C.; Umutlu, L. FDG PET/MRI vs. PET/CT for whole-body staging in patients with recurrent malignancies of the female pelvis: Initial results. Eur. J. Nucl. Med. Mol. Imaging 2015, 42, 56–65.
27. Narva, S.I.; Seppänen, M.P.; Raiko, J.R.H.; Forsback, S.J.; Orte, K.J.; Virtanen, J.M.; Hynninen, J.; Hietanen, S. Imaging of Tumor Hypoxia With 18F-EF5 PET/MRI in Cervical Cancer. Clin. Nucl. Med. 2021, 46, 952–957.
28. Kidd, E.A.; Grigsby, P.W. Intratumoral metabolic heterogeneity of cervical cancer. Clin. Cancer Res. 2008, 14, 5236–5241.

29. Sapienza, L.G.; Salcedo, M.P.; Ning, M.S.; Jhingran, A.; Klopp, A.H.; Calsavara, V.F.; Schmeler, K.M.; Leite Gomes, M.J.; de Freitas Carvalho, E.; Baiocchi, G. Pelvic Insufficiency Fractures After External Beam Radiation Therapy for Gynecologic Cancers: A Meta-analysis and Meta-regression of 3929 Patients. Int. J. Radiat. Oncol. Biol. Phys. 2020, 106, 475–484.
30. Azumi, M.; Matsumoto, M.; Suzuki, K.; Sasaki, R.; Ueno, Y.; Nogami, M.; Terai, Y. PET/MRI is useful for early detection of pelvic insufficiency fractures after radiotherapy for cervical cancer. Oncol. Lett. 2021, 22, 776.
31. Kidd, E.A.; El Naqa, I.; Siegel, B.A.; Dehdashti, F.; Grigsby, P.W. FDG-PET-based prognostic nomograms for locally advanced cervical cancer. Gynecol. Oncol. 2012, 127, 136–140.
32. Kidd, E.A.; Siegel, B.A.; Dehdashti, F.; Grigsby, P.W. The standardized uptake value for F-18 fluorodeoxyglucose is a sensitive predictive biomarker for cervical cancer treatment response and survival. Cancer 2007, 110, 1738–1744.
33. Zhao, Q.; Feng, Y.; Mao, X.; Qie, M. Prognostic value of fluorine-18-fluorodeoxyglucose positron emission tomography or PET-computed tomography in cervical cancer: A meta-analysis. Int. J. Gynecol. Cancer 2013, 23, 1184–1190.
34. Ho, J.C.; Allen, P.K.; Bhosale, P.R.; Rauch, G.M.; Fuller, C.D.; Mohamed, A.S.; Frumovitz, M.; Jhingran, A.; Klopp, A.H. Diffusion-Weighted Magnetic Resonance Imaging as a Predictor of Outcome in Cervical Cancer After Chemoradiation. Int. J. Radiat. Oncol. Biol. Phys. 2017, 97, 546–553.
35. Das, S.; Chandramohan, A.; Reddy, J.K.; Mukhopadhyay, S.; Kumar, R.M.; Isiah, R.; John, S.; Oommen, R.; Jeyaseelan, V. Role of conventional and diffusion weighted MRI in predicting treatment response after low dose radiation and chemotherapy in locally advanced carcinoma cervix. Radiother. Oncol. 2015, 117, 288–293.
36. Park, J.J.; Kim, C.K.; Park, B.K. Prediction of disease progression following concurrent chemoradiotherapy for uterine cervical cancer: Value of post-treatment diffusion-weighted imaging. Eur. Radiol. 2016, 26, 3272–3279.
37. Park, J.J.; Kim, C.K.; Park, S.Y.; Park, B.K.; Kim, B. Value of diffusion-weighted imaging in predicting parametrial invasion in stage IA2-IIA cervical cancer. Eur. Radiol. 2014, 24, 1081–1088.
38. Olsen, J.R.; Esthappan, J.; DeWees, T.; Narra, V.R.; Dehdashti, F.; Siegel, B.A.; Schwarz, J.K.; Grigsby, P.W. Tumor volume and subvolume concordance between FDG-PET/CT and diffusion-weighted MRI for squamous cell carcinoma of the cervix. J. Magn. Reson. Imaging 2013, 37, 431–434.
39. Kidd, E.A.; Spencer, C.R.; Huettner, P.C.; Siegel, B.A.; Dehdashti, F.; Rader, J.S.; Grigsby, P.W. Cervical cancer histology and tumor differentiation affect 18F-fluorodeoxyglucose uptake. Cancer 2009, 115, 3548–3554.

40. Mendez, L.E.; Manci, N.; Cantuaria, G.; Gomez-Marin, O.; Penalver, M.; Braunschweiger, P.; Nadji, M. Expression of glucose transporter-1 in cervical cancer and its precursors. Gynecol. Oncol. 2002, 86, 138–143.
41. Yen, T.C.; See, L.C.; Lai, C.H.; Yah-Huei, C.W.; Ng, K.K.; Ma, S.Y.; Lin, W.J.; Chen, J.T.; Chen, W.J.; Lai, C.R.; et al. 18F-FDG uptake in squamous cell carcinoma of the cervix is correlated with glucose transporter 1 expression. J. Nucl. Med. 2004, 45, 22–29.
42. Brandmaier, P.; Purz, S.; Bremicker, K.; Höckel, M.; Barthel, H.; Kluge, R.; Kahn, T.; Sabri, O.; Stumpp, P. Simultaneous FDG-PET/MRI: Correlation of Apparent Diffusion Coefficient (ADC) and Standardized Uptake Value (SUV) in Primary and Recurrent Cervical Cancer. PLoS ONE 2015, 10, e0141684.
43. Grueneisen, J.; Schaarschmidt, B.M.; Heubner, M.; Aktas, B.; Kinner, S.; Forsting, M.; Lauenstein, T.; Ruhlmann, V.; Umutlu, L. Integrated PET/MRI for whole-body staging of patients with primary cervical cancer: Preliminary results. Eur. J. Nucl. Med. Mol. Imaging 2015, 42, 1814–1824.
44. Ho, K.C.; Lin, G.; Wang, J.J.; Lai, C.H.; Chang, C.J.; Yen, T.C. Correlation of apparent diffusion coefficients measured by 3T diffusion-weighted MRI and SUV from FDG PET/CT in primary cervical cancer. Eur. J. Nucl. Med. Mol. Imaging 2009, 36, 200–208.
45. Surov, A.; Meyer, H.J.; Schob, S.; Höhn, A.K.; Bremicker, K.; Exner, M.; Stumpp, P.; Purz, S. Parameters of simultaneous 18F-FDG-PET/MRI predict tumor stage and several histopathological features in uterine cervical cancer. Oncotarget 2017, 8, 28285–28296.
46. Xu, W.; Yu, S.; Xin, J.; Guo, Q. Relationship of 18F-FDG PET/CT metabolic, clinical and pathological characteristics of primary squamous cell carcinoma of the cervix. J. Investig. Med. 2016, 64, 1246–1251.
47. Du, S.; Sun, H.; Gao, S.; Xin, J.; Lu, Z.; Chen, Z.; Pan, S.; Guo, Q. Relationship between 18F-FDG PET metabolic parameters and MRI intravoxel incoherent motion (IVIM) histogram parameters and their correlations with clinicopathological features of cervical cancer: Evidence from integrated PET/MRI. Clin. Radiol. 2019, 74, 178–186.
48. Floberg, J.M.; Fowler, K.J.; Fuser, D.; DeWees, T.A.; Dehdashti, F.; Siegel, B.A.; Wahl, R.L.; Schwarz, J.K.; Grigsby, P.W. Spatial relationship of 2-deoxy-2--fluoro-D-glucose positron emission tomography and magnetic resonance diffusion imaging metrics in cervical cancer. EJNMMI Res. 2018, 8, 52.
49. Umutlu, L.; Nensa, F.; Demircioglu, A.; Antoch, G.; Herrmann, K.; Forsting, M.; Grueneisen, J.S. Radiomics Analysis of Multiparametric PET/MRI for N- and M-Staging in Patients with Primary Cervical Cancer. Rofo 2020, 192, 754–763.
50. Meyer, H.J.; Purz, S.; Sabri, O.; Surov, A. Cervical Cancer: Associations between Metabolic Parameters and Whole Lesion Histogram Analysis Derived from Simultaneous 18F-FDG-

PET/MRI. Contrast Media Mol. Imaging 2018, 2018, 5063285.

51. Vojtíšek, R.; Baxa, J.; Kovářová, P.; Almortaza, A.; Hošek, P.; Sukovská, E.; Tupý, R.; Ferda, J.; Fínek, J. Prediction of treatment response in patients with locally advanced cervical cancer using midtreatment PET/MRI during concurrent chemoradiotherapy. Strahlenther. Onkol. 2021, 197, 494–504.
52. Ahangari, S.; Hansen, N.L.; Olin, A.B.; Nøttrup, T.J.; Ryssel, H.; Berthelsen, A.K.; Löfgren, J.; Loft, A.; Vogelius, I.R.; Schnack, T.; et al. Toward PET/MRI as one-stop shop for radiotherapy planning in cervical cancer patients. Acta Oncol. 2021, 60, 1045–1053.
53. Kim, S.K.; Choi, H.J.; Park, S.Y.; Lee, H.Y.; Seo, S.S.; Yoo, C.W.; Jung, D.C.; Kang, S.; Cho, K.S. Additional value of MR/PET fusion compared with PET/CT in the detection of lymph node metastases in cervical cancer patients. Eur. J. Cancer 2009, 45, 2103–2109.
54. Ahangari, S.; Littrup Andersen, F.; Liv Hansen, N.; Jakobi Nøttrup, T.; Berthelsen, A.K.; Folsted Kallehauge, J.; Richter Vogelius, I.; Kjaer, A.; Espe Hansen, A.; Fischer, B.M. Multi-parametric PET/MRI for enhanced tumor characterization of patients with cervical cancer. Eur. J. Hybrid Imaging 2022, 6, 7.
55. Gong, J.; Liu, H.; Bao, Z.; Bian, L.; Li, X.; Meng, Y. Relative clinical utility of simultaneous 18F-fluorodeoxyglucose PET/MRI and PET/CT for preoperative cervical cancer diagnosis. J. Int. Med. Res. 2021, 49, 3000605211019190.
56. Xin, J.; Ma, Q.; Guo, Q.; Sun, H.; Zhang, S.; Liu, C.; Zhai, W. PET/MRI with diagnostic MR sequences vs PET/CT in the detection of abdominal and pelvic cancer. Eur. J. Radiol. 2016, 85, 751–759.
57. Queiroz, M.A.; Kubik-Huch, R.A.; Hauser, N.; Freiwald-Chilla, B.; von Schulthess, G.; Froehlich, J.M.; Veit-Haibach, P. PET/MRI and PET/CT in advanced gynaecological tumours: Initial experience and comparison. Eur. Radiol. 2015, 25, 2222–2230.
58. Spick, C.; Herrmann, K.; Czernin, J. 18F-FDG PET/CT and PET/MRI Perform Equally Well in Cancer: Evidence from Studies on More Than 2,300 Patients. J. Nucl. Med. 2016, 57, 420–430.
59. Grueneisen, J.; Schaarschmidt, B.M.; Beiderwellen, K.; Schulze-Hagen, A.; Heubner, M.; Kinner, S.; Forsting, M.; Lauenstein, T.; Ruhlmann, V.; Umutlu, L. Diagnostic value of diffusion-weighted imaging in simultaneous 18F-FDG PET/MR imaging for whole-body staging of women with pelvic malignancies. J. Nucl. Med. 2014, 55, 1930–1935.
60. Schwartz, M.; Gavane, S.C.; Bou-Ayache, J.; Kolev, V.; Zakashansky, K.; Prasad-Hayes, M.; Taouli, B.; Chuang, L.; Kostakoglu, L. Feasibility and diagnostic performance of hybrid PET/MRI compared with PET/CT for gynecological malignancies: A prospective pilot study. Abdom. Radiol. 2018, 43, 3462–3467.

61. Nakajo, K.; Tatsumi, M.; Inoue, A.; Isohashi, K.; Higuchi, I.; Kato, H.; Imaizumi, M.; Enomoto, T.; Shimosegawa, E.; Kimura, T.; et al. Diagnostic performance of fluorodeoxyglucose positron emission tomography/magnetic resonance imaging fusion images of gynecological malignant tumors: Comparison with positron emission tomography/computed tomography. Jpn. J. Radiol. 2010, 28, 95–100.